The Bose–Hubbard model with squeezed dissipation

Article (Accepted Version)

The Bose–Hubbard model with squeezed dissipation

2015 J. Phys. B: At. Mol. Opt. Phys. 48 055302

(http://iopscience.iop.org/0953-4075/48/5/055302)

IOP Publishing Journal of Physics B: Atomic, Molecular and Optical Physics
J. Phys. B: At. Mol. Opt. Phys. **48** (2015) 055302 (9pp) doi:10.1088/0953-4075/48/5/055302

The Bose–Hubbard model with squeezed dissipation

Fernando Quijandría[1], Uta Naether[1], Diego Porras[2], Juan José García-Ripoll[3] and David Zueco[1,4]

[1] Instituto de Ciencia de Materiales de Aragón y Departamento de Física de la Materia Condensada, CSIC-Universidad de Zaragoza, Zaragoza, E-50012, Spain
[2] Department of Physics and Astronomy, University of Sussex, Brighton BN1 9QH, UK
[3] Instituto de Física Fundamental, IFF-CSIC, Serrano 113-bis, Madrid E-28006, Spain
[4] Fundación ARAID, Paseo María Agustín 36, Zaragoza E-50004, Spain

E-mail: fquijan@unizar.es

Received 24 October 2014, revised 16 December 2014
Accepted for publication 2 January 2015
Published 30 January 2015

Abstract

The stationary properties of the Bose–Hubbard model under squeezed dissipation are investigated. The dissipative model does not possess a $U(1)$ symmetry but conserves parity. We find that $\langle a_j \rangle = 0$ always holds, so no symmetry breaking occurs. Without the onsite repulsion, the linear case is known to be critical. At the critical point the system freezes to an EPR state with infinite two mode entanglement. We show here that the correlations are rapidly destroyed whenever the repulsion is switched on. As we increase the latter, the system approaches a thermal state with an effective temperature defined in terms of the squeezing parameter in the dissipators. We characterize this transition by means of a Gutzwiller ansatz and the Gaussian Hartree–Fock–Bogoliubov approximation.

Keywords: dissipative dynamics, Bose–Hubbard, Gutzwiller ansatz, Gaussian approximation, squeezing

(Some figures may appear in colour only in the online journal)

1. Introduction

Optical realizations of many body phases of matter constitute seminal implementations of quantum simulators [1]. Cold atoms in optical lattices are a key example in the simulation of strongly correlated systems. Quantum phase transitions as well as non-equilibrium dynamics are impressive demonstrations of such fine tuned testbed experimental setups. More recently, solid state realizations are expected to provide new architectures for the exploration of non-trivial many body physics [2]. The isolation in cold atoms is usually assumed and well reproduced in experiments. Thus, unitary evolution and closed system equilibration are reported.

However, such a good isolation is not always possible, which is (mostly) considered as a drawback. On the other hand, the unavoidable interaction with the environment motivates the search for novel phases of many body stationary dynamics including driving and dissipation. An excellent arena for dealing with such a situation are man-made realizations as the ones mentioned above. There, not only the interactions can be engineered but also the coupling with the environment. Roughly, the equilibrium statistical mechanics is now extended considering the bath and the type of system-environment interaction. This *extra* dependence leads to non-thermal stationary states $\varrho \neq \mathrm{e}^{-\beta H_s}$ with novel equilibrium phases [3–15].

Many body phases for interacting bosons on the lattice, as the ones implemented in condensates, cold atoms or circuits, can be understood with the Bose–Hubbard (BH) model [1, 16–19]. Here, we study the equilibrium properties of this model, when it is driven by squeezed dissipation. The model is not analytically solvable, thus we have performed numerical simulations. These are exact for the single and two site cases. We have also made use of the Hartree–Fock–Bogoliubov (HFB) approximation and Gutzwiller ansatz to deal with the many body problem. From the physics point of view, squeezed noise provides long-range correlations, producing even a critical point in Gaussian models [7, 15]. This long

order correlation competes with the self-interaction of the model (characterized in this work by the strength U). After an extensive study, the phenomenology that we find is rather simple. Under squeezed dissipation, the system does not condensate. For zero onsite repulsion, the system has a critical point. It equilibrates to an EPR state. Whenever this repulsion is switch on, the correlations are destroyed and the system approaches a thermal state with a synthetic temperature related to the squeezing.

The rest of the paper is organized as follows. In section 2 the model and its dissipative evolution is presented. In section 3 we introduce the two approximations used throughout this work, namely, the HFB approximation and the Gutzwiller ansatz. Also, we present the exact numerical solver and introduce how to compute multiparticle squeezing. Section 4 summarizes our results. Some conclusions are written in section 5 and additional technical details have been left for the appendices.

2. Model and its dissipative evolution

In this work we discuss stationary solutions ($\partial_\tau \varrho_{\rm eq} = 0$) of Lindblad-like master equations:

$$\mathrm{d}_\tau \varrho = -\frac{\mathrm{i}}{\hbar}\left[\bar{H}_{\rm S}, \varrho\right] + \gamma \sum_j^N L_j \varrho L_j^\dagger - \frac{1}{2}\left\{L_j^\dagger L_j, \varrho\right\}. \quad (1)$$

Here, ϱ is the reduced density matrix, $\bar{H}_{\rm S}$ is the system Hamiltonian, the operators L_j are the dissipators, $\{\ ,\ \}$ stands for the anticommutator and γ is the decay rate. In this work we discuss the competition between Hamiltonian and dissipative dynamics. For convenience, and since we are interested in stationary solutions, we introduce the time scale $t = \gamma\tau$. This, in turn, allows us to define the dimensionless Hamiltonian $H_{\rm S} = \bar{H}_{\rm S}/(\hbar\gamma)$.

The Lindblad-like form, also known as Gorini–Kossakowski–Sudarshan–Lindblad equation (to credit), is the most general Markovian evolution [20]. An evolution like (1) can be derived from a system-bath Hamiltonian. In this approach, the system, with Hamiltonian $H_{\rm S}$, is surrounded by a bath ($H_{\rm b}$) formed by a continuum set of modes. Both system and bath are coupled yielding $H = H_{\rm S} + H_{\rm b} + H_{\rm I}$, with $H_{\rm I}$ the interaction Hamiltonian. After tracing out the bath modes and assuming weak coupling, the dynamics for the reduced density matrix ϱ is given by (1). Weak coupling regime means that the dynamics is governed by the system Hamiltonian, the coupling to the bath being a perturbation. The weak coupling limit is well justified whenever the bath correlation functions decay sufficiently fast [20]. Although these conditions seem to be quite restrictive, equations like (1) are justified and used in a lot of cases of interest.

When one faces such a situation, typically, the dissipators are such that the stationary state coincides with Gibbs $\rho_{\rm eq} \sim \mathrm{e}^{-\beta H}$ ([21] section 3.2.2). This is a nice property connecting non-equilibrium dynamics with *standard* thermal physics. Exceptions to the latter come whenever the coupling can not be considered weak [22] or by deforming the coupling via, e.g., driving. If the system-bath coupling leaves the Markovian-weak limit the evolution is in general much more complicated than (1) [21]. However, it turns out that via the inclusion of driving fields and ancillary systems the system-bath can be in this weak limit and at the same time possess a non-thermal effective dynamics. In order to achieve this, some dissipator engineering is required. This is the case that we are going to discuss here. We will still assume a Lindblad form but the dissipators are going to be *non-thermal*, i.e. such that $\varrho_{\rm eq} \neq \mathrm{e}^{-\beta H}$.

2.1. BH in a squeezed dissipator

We study the one-dimensional BH model

$$H_{\rm S} = \sum_j^N \omega n_j + U n_j\left(n_j - 1\right) + J\left(a_j^\dagger a_{j+1} + \text{h.c.}\right), \quad (2)$$

here $n_j = a_j^\dagger a_j$ with a_j ($a_j^\dagger$) the annihilation (creation) bosonic operators on site j ($[a_j, a_{j'}^\dagger] = \delta_{jj'}$). The onsite repulsion has an strength U and the intersite hopping strength is J.

We concentrate on both local and linear dissipators:

$$L_j = a_j + \eta \mathrm{e}^{\mathrm{i}q j} a_j^\dagger. \quad (3)$$

In [15] it is shown that such dissipators can be constructed by using qubits as ancillary systems and driving the side-bands. This dissipation-like mechanism was also proven to drive free bosonic ($U = 0$) Hamiltonians to a critical state [7, 15]. Thus, the model we present here is both physically realizable and has its interest in many-body physics driven by dissipation. By making $\eta = 0$ we obtain the typical loss mechanism $L_j = a_j$ [19, 23, 24] which leads to the trivial zero excitations vacuum state $\varrho_{\rm eq} = \bigotimes_j |0\rangle_j\langle 0|_j$ with $a_j|0\rangle_j = 0$.

3. Methods

We discuss here the methods used for solving (1), with Hamiltonian (2) and dissipators (3) and introduce the squeezing.

3.1. HFB approximation

In the non-interacting case ($U = 0$) equation (1) is easily solvable by working with second moments ($\langle a_i a_j\rangle = \mathrm{Tr}\,(\varrho a_i a_j)$, $\langle a_i^\dagger a_j\rangle = \mathrm{Tr}\,(\varrho a_i^\dagger a_j)$). The equations for the latter form a closed set. In this limit, the system is Gaussian. However, whenever $U \neq 0$ the equations for the moments form an infinite hierarchy, coupling correlators of higher orders. This hierarchy needs to be cut. In order to do so, we introduce the HFB approximation. This is a *Gaussian* ansatz which consists in considering the cumulant expansion up to second order. As argued, this is exact if $U = 0$. This approximation has been tested in a variety of situations as you can read in [25–30]. We show below, section 4, that the HFB approximation is sufficient for describing the main phenomenology.

Within the Gaussian ansatz, averages can be computed invoking Wick's theorem. For our purposes, it is sufficient to consider the formula:

$$\langle X_1X_2X_3X_4\rangle = \sigma_{12}\sigma_{34} + \sigma_{13}\sigma_{24} + \sigma_{14}\sigma_{23} - 2\langle X_1\rangle\langle X_2\rangle\langle X_3\rangle\langle X_4\rangle, \tag{4}$$

where $\sigma_{ij} = \langle X_iX_j\rangle$ and $\langle\cdot\rangle = \mathrm{Tr}(\cdot\ \varrho)$. Writing these higher order correlators as a function of first and second order ones permits to find a closed set of equations. Some algebra yields the equations for the field averages (first moments) (cf equations (1)–(3)):

$$\mathrm{d}_t\langle a_i\rangle = -\mathrm{i}\Big(\omega + 4U\Big(\langle n_i\rangle - |\langle a_i\rangle|^2\Big)\Big)\langle a_i\rangle - 2\mathrm{i}U\langle a_i^2\rangle\langle a_i\rangle^* - \mathrm{i}J\Big(\langle a_{i-1}\rangle + \langle a_{i+1}\rangle\Big) - \frac{1}{2}\Big(1-\eta^2\Big)\langle a_i\rangle. \tag{5}$$

For the second moments $X_{ij} := \langle a_i^\dagger a_j\rangle$ and $Y_{ij} := \langle a_i a_j\rangle$ we find that

$$\begin{aligned}\mathrm{d}_tX_{ij} = {}&\mathrm{i}U\Big(Y_{ii}^*Y_{ij} + 2X_{ij}X_{ii} - Y_{ij}^*Y_{jj} - 2X_{ij}X_{jj} \\ &- 2\langle a_i\rangle^{*2}\langle a_i\rangle\Big\langle a_j\Big\rangle + 2\langle a_i\rangle^*\Big\langle a_j\Big\rangle^*\Big\langle a_j\Big\rangle^2\Big) \\ &+ \mathrm{i}J\Big(X_{i-1,j} - X_{i,j+1} + X_{i+1,j} - X_{i,j-1}\Big) \\ &- \Big(1-\eta^2\Big)X_{ij} + \eta^2\delta_{ij},\end{aligned} \tag{6}$$

and

$$\begin{aligned}\mathrm{d}_tY_{ij} = {}&-2\mathrm{i}\omega Y_{ij} - \mathrm{i}U\Big(2X_{ji}Y_{jj} + 4X_{jj}Y_{ij} + 2X_{ij}Y_{ii} + 4X_{ii}Y_{ij} \\ &+ 4\delta_{ij}Y_{jj} - 4\Big\langle a_j\Big\rangle^*\langle a_i\rangle\Big\langle a_j\Big\rangle^2 - 4\langle a_i\rangle^*\Big\langle a_j\Big\rangle\langle a_i\rangle^2\Big) \\ &- \mathrm{i}J\Big(Y_{i,j+1} + Y_{j,i+1} + Y_{i,j-1} + Y_{j,i-1}\Big) \\ &- \Big(1-\eta^2\Big)Y_{ij} - \eta\mathrm{e}^{\mathrm{i}\varphi j}\delta_{ij}.\end{aligned} \tag{7}$$

With these equations at hand it is possible to solve the nonlinear set of $N \times N$ equations numerically for a reasonably large N.

Simpler than the HFB is the so-called classical approximation. The latter consists in replacing $\langle a_i^2\rangle \to \langle a_i\rangle^2$. In the absence of dissipation, this yields the discrete nonlinear Schrödinger equation [31]. In this classical approximation, the fourth term in equation (5) simplifies to $-2\mathrm{i}U|\langle a_i\rangle|^2\langle a_i\rangle$. Then, the equations for $\partial_t\langle a_i\rangle$ become a closed set of nonlinear equations. The second moments play no role at all because, by definition, they are just the square of the first moments. The classical approximation can indeed capture relevant physics, e.g. the Mott-superfluid transition in the BH model. However, in our case, equation (5) with the aforementioned replacement yields the trivial $\langle a_i\rangle_{\varrho_{\mathrm{eq}}} = 0$ stationary state (through the text we use the notation $\langle\cdot\rangle_{\varrho_{\mathrm{eq}}} \equiv \mathrm{Tr}(\cdot\ \varrho_{\mathrm{eq}})$). As a consequence of this, we have that $\langle a_i^2\rangle_{\varrho_{\mathrm{eq}}} = \langle a_i\rangle^2_{\varrho_{\mathrm{eq}}} = 0$. Therefore, the HFB marks the first nontrivial approximation for dealing with the BH model with squeezed dissipation.

3.2. Gutzwiller ansatz

The Gutzwiller ansatz imposes a factorized form for the density matrix:

$$\varrho = \bigotimes_j^N \varrho_j. \tag{8}$$

Assuming translational invariance ($N \to \infty$ or periodic boundary conditions), the problem is reduced to a single site, nonlinear master equation that can be numerically solved, imposing a cuttoff in the Fock space dimension. Within the factorized form (8) and noticing that $\mathrm{tr}(\varrho_j) = 1$ ($\mathrm{tr}(\partial_t\rho_j) = 0$), equation (1) yields the following nonlinear equation

$$\begin{aligned}\mathrm{d}\varrho_j = {}&-\mathrm{i}\Big[\omega n_j + Un_j\Big(n_j - 1\Big) + J\Big\langle a_j\Big\rangle a_j^\dagger + \mathrm{h.c.}, \varrho_j\Big] \\ &+ L_j\varrho_jL_j^\dagger - \frac{1}{2}\Big\{L_j^\dagger L_j, \varrho_j\Big\}\end{aligned} \tag{9}$$

with $\langle a_j\rangle \equiv \mathrm{tr}(a_j\varrho_j)$. We obtain a set of of nonlinear equations for the density matrix elements $[\varrho_j]_{nm}$ and integrate to find their time evolution. In the long time dynamics the stationary solution is found.

The factorized ansatz, equation (8), catches only short distance correlated states. However, the interacting (local) part $Un_j(n_j - 1)$ is fully taken into account. In this sense, Gutzwiller is complementary to the HFB approximation.

3.3. Numerical solution

These two approximations will be corroborated against *exact* numerical solutions. Notice that for one and two sites ($N = 1$, 2) the Lindblad evolution can be solved numerically. In this paper we have performed numerical simulations using the quantum optics toolbox for MATLAB [32]. The truncation of the Fock space dimension, with a good degree of confidence, follows from the comparison of numerical results with exact analytical predictions for the non-interacting model ($U = 0$) (cf figure 1 (blue lines)).

3.4. Squeezing

It will be useful for us to characterize the amount of *quadrature squeezing*. For a N-mode system with annihilation operators a_j, $j = 1,...,N$, the corresponding Hermitian quadrature operators are defined as follows

$$X_i = \frac{1}{\sqrt{2}}\Big(a_i^\dagger + a_i\Big), \tag{10}$$

$$P_i = \frac{\mathrm{i}}{\sqrt{2}}\Big(a_i^\dagger - a_i\Big). \tag{11}$$

Squeezing involves the second moments of the quadrature operators. These in turn define the covariance matrix γ

$$\gamma_{ij} = \frac{1}{2}\Big\langle R_iR_j + R_jR_i\Big\rangle - \langle R_i\rangle\Big\langle R_j\Big\rangle, \tag{12}$$

with $R = (X_1, P_1, X_2, P_2,..., X_N, P_N)$. Following [33] we formulate the squeezing criterion as follows: *a multimode system is said to be squeezed whenever the smallest eigenvalue of its*

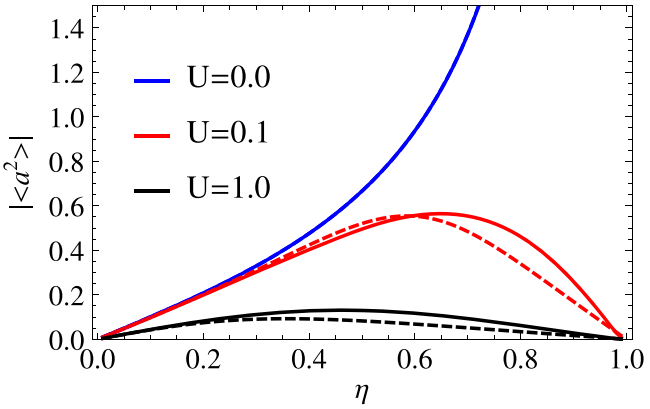

Figure 1. Absolute value of $\langle a^2\rangle$ as a function of η for different values of U. We compare the numerical solution (solid line) and the HFB approximation (dashed line). The numerical solution is done by using $N_C = 40$, where N_C is the maximum number of Fock states considered. The rest of parameters are $\Gamma = 1$, $\omega = 0$ and $q = \pi/2$.

covariance matrix is smaller than 1/2. We should point out that the 'size' of this minimum eigenvalue and the squeezing are complementary quantities. Having a big amount of squeezing implies that the minimum eigenvalue is very small ($\ll$1/2). For example, when we say that there is an infinite amount of squeezing, we refer to the limiting situation in which the smallest eigenvalue of the covariance matrix approaches to zero.

4. Results

In the following, periodic boundary conditions are assumed for the HFB approximation while translational invariance is assumed for the Gutzwiller ansatz.

4.1. Non-interacting case ($U = 0$)

The limit $U = 0$ was studied in [15]. In a nutshell, dissipation-induced critical behaviour was found there. In momentum-space, the role of the Lindblad operators in the quantum master equation (QME) was to entangle pairs of modes whose sum of momenta was equal to the driving phase q. Writing (1) in momentum space ($a_k = N^{-1/2}\sum_j e^{-ijk}a_j$) yields

$$d_t\varrho = \sum_k -i\omega_k\left[a_k^\dagger a_k, \varrho\right] + \frac{1}{2}\left(2b_k\varrho b_k^\dagger - \left\{b_k^\dagger b_k, \varrho\right\}\right) \quad (13)$$

with

$$b_k = a_k + \eta a_{-k+q}^\dagger, \quad (14)$$

i.e., the modes b_k are two mode squeezed operators, and $\omega_k = \omega + 2J\cos(k)$ the normal frequencies.

By looking at the master equation (13) and with a *correct* choice of the system parameters: $\omega_k + \omega_{-k+q} = 0$ we readily see that these two modes $(k, -k+q)$ become maximally entangled. For the rest, a limiting case can be described. Whenever ω_k, $\omega_{-k+q} \gg \Gamma$ we can perform the rotating wave approximation (RWA) for the dissipators and the modes will reach a thermal state, $\varrho \sim e^{-\beta^* a_k^\dagger a_k}$ with an effective temperature, β^* given below by (17). The above argument will be elaborated in the following two sections for the more general case of $U \neq 0$ (see 4.2 (for the single site) and 4.3 for the many body problem).

4.2. Single site case: transition to a thermal state

Let us now move to the interacting case for a single site. We anticipate here the main result, which is exportable to the many-body part. There is a competition between the boson-boson interaction, with strength U, and the squeezed dissipators L_j. In the limit: ω, $U \ll 1$, $\varrho_{\rm eq}$ relaxes to a squeezed vacuum state. On the other hand, if ω, $U \gg 1$, then $\varrho_{\rm eq} \sim \prod_j e^{-\beta^*\omega n_j}$ with $\beta^* = 1/T^*$, an effective temperature (to be defined below). This trade off explains the equilibrium statistics of the model (1) with (2) and (3). Moreover, the parity symmetry $a_j \to -a_j$ is never broken, finding always that $\langle a_j\rangle = 0$. Let us check this picture.

Making $H_S = 0$, the evolution (1) is given by $\partial_t\varrho = L\varrho L^\dagger - 1/2\{LL^\dagger, \varrho\}$, with $L = a + \eta e^{iq}a^\dagger$ (for the single site). Therefore $\varrho_{\rm eq} = |\xi\rangle\langle\xi|$, with $L|\xi\rangle = 0$, i.e. the vacuum squeezed state. On the other hand, if ω, $U \gg 1$, it is convenient to work in the interaction picture (with respect to the H_S). We have that

$$VaV^\dagger = \sum_n e^{-i(\omega+2nU)t}|n\rangle\langle n|a \quad (15)$$

with $V = \exp[i(\omega n + Un(n-1))t]$, i.e., the Hamiltonian rotates each Fock state with a different phase. Using a rotating wave-like argument we can expect that the time-dependent terms average to zero. Conserving only the non-rotating terms we have that the QME (1) can be approximated by:

$$d_t\varrho = \frac{1}{2}\left(2a\varrho a^\dagger - \{a^\dagger a, \varrho\}\right) + \frac{\eta^2}{2}\left(2a^\dagger\varrho a - \{aa^\dagger, \varrho\}\right). \quad (16)$$

Identifying $\eta^2 = \bar{n}(\omega)/(1 + \bar{n}(\omega))$, with $\bar{n}(\omega)$ the Bose distribution $\bar{n}(\omega) = 1/(e^{\beta\hbar\omega} - 1)$, the above matches the dissipators for a damped harmonic oscillator in a thermal bath with effective temperature

$$\beta^*\omega = -2\ln\eta. \quad (17)$$

The above argument can be validated and refined. It is not hard to realize that, independently of the value of U, we have that:

$$\langle n\rangle_{\varrho_{\rm eq}} \equiv \langle a^\dagger a\rangle_{\varrho_{\rm eq}} = \frac{\eta^2}{1-\eta^2}. \quad (18)$$

Notice that by using (17) in (18) we obtain the thermal Bose distribution $\langle n\rangle_{\varrho_{\rm eq}} = (e^{\beta^*\omega} - 1)^{-1}$. Therefore, for the boson number, the state is as would be a thermal state with the temperature predicted by the previous simple argument, equation (17).

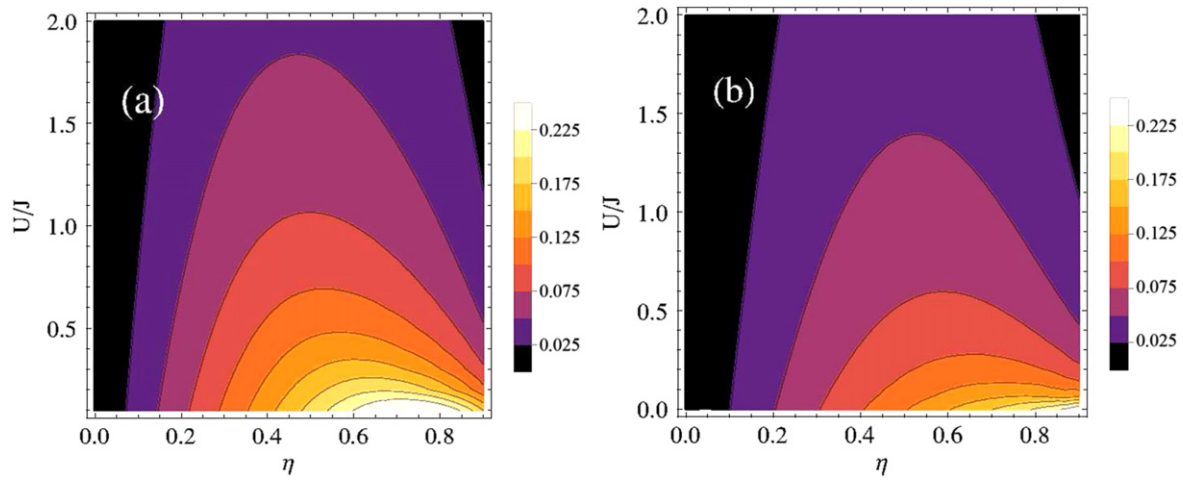

Figure 2. (a) and (b): $|\langle a_j^2\rangle|$ as a function of η and U/J for the HFB and the Gutzwiller ansatz, respectively. For both, HFB and Gutzwiller, we have chosen: $\omega = -2J$ and $q = 0$. The HFB result considers a linear array with 10 sites and periodic boundary conditions. For the Gutzwiller solution we have taken a photon cut-off $N_C = 60$.

In obtaining a dynamical equation for other variances, as $\langle a\rangle$ and $\langle a^2\rangle$ we find an infinity hierarchy of equations involving higher order averages as $\langle (a^\dagger)^n a^m\rangle$. We make use of the HFB or Gaussian approximation, as explained in section 3.1. The HFB can be justified *a priori* as follows. We expect to obtain the Gaussian thermal state $\varrho_{\rm eq} \sim {\rm e}^{-\beta^* a^\dagger a}$ by increasing U. On the other hand, whenever $U = 0$, the HFB is exact.

Particularizing equations (5) and (8) to the single site case we can write a system of differential equations for $\langle a\rangle$ and $\langle a^2\rangle$

$$\mathrm{d}_t\langle a\rangle = \left(-\mathrm{i}\omega - \frac{1}{2}\left(1-\eta^2\right)\right)\langle a\rangle - 2\mathrm{i}U\left(2\langle n\rangle\langle a\rangle + \langle a^2\rangle\langle a\rangle^* - 2\langle a\rangle^*\langle a\rangle^2\right), \tag{19}$$

$$\mathrm{d}_t\langle a\rangle = (-\mathrm{i}(2\omega + 2U + 12U\langle n\rangle) - \left(1-\eta^2\right))\langle a^2\rangle + 8\mathrm{i}U\langle a\rangle^*\langle a\rangle^3 - \eta\mathrm{e}^{\mathrm{i}q}. \tag{20}$$

This, together with (18), can be solved for its steady-state.

Apart from the aforementioned transition to a thermal state, the other key result in this paper is the following. We always find that (see appendix A for technical details):

$$\langle a\rangle_{\varrho_{\rm eq}} = 0. \tag{21}$$

Therefore, for the single site case and within the HFB approximation, the parity symmetry is never broken. Further discussion will be given in 4.3.

The steady-state solution for $\langle a^2\rangle$ is given by

$$\langle a^2\rangle_{\varrho_{\rm eq}} = \frac{-\eta\mathrm{e}^{\mathrm{i}q}}{\left(1-\eta^2\right) + \mathrm{i}2\left[U\left(6\langle n\rangle_{\varrho_{\rm eq}} + 1\right) + \omega\right]}. \tag{22}$$

We see that $\langle a^2\rangle_{\varrho_{\rm eq}}$ approaches zero as $U \gg 1$, while $\langle a\rangle_{\varrho_{\rm eq}}$ and $\langle n\rangle_{\varrho_{\rm eq}}$ always equal their thermal averages (cf equations (18) and (21)). Therefore, the Gaussian approximation, in the limit $U \gg 1$, matches the thermal state $\varrho_{\rm eq} \sim {\rm e}^{-\beta^* a^\dagger a}$, as expected.

To validate all this, we resort to numerical simulations, as explained in 3.3. In figure 1 we show, first, that the HFB captures well the numerical result. Besides, we observe that the squeezing grows with η whenever $U = 0$ [15]. As soon as $U > 0$ the state approaches a thermal state with temperature $\beta^* \sim -\log\eta$ (cf equation (17)). Therefore, η favours both squeezing ($U = 0$) and high-T thermal states ($U \neq 0$). From this trade-off the maximum for $\langle a^2\rangle_{\varrho_{\rm eq}}$ in figure 1 is understood.

4.3. Many body

Equipped with the last results, we move to the many body, i.e., more than one site. In this case, a numerical solution becomes very costly due to the violent growth of the total Hilbert space size. This renders the general many body problem non-tractable numerically. In turn, we have the Gaussian approximation which in the single site case works reasonably well (cf figure 1). In appendix B we check the validity of the HFB for the two site case in comparison with the exact numerics. Besides, the HFB approximation will be complemented with a Gutzwiller ansatz. Combining both approaches we should be able to capture the main physics.

We plot in figures 2 and 3 $|\langle a_j^2\rangle|$ and $\langle a_j^\dagger a_j\rangle$ respectively, comparing both approximations. For the HFB, systems with $N = 10$ sites have been considered. We remind that periodic boundary conditions were used, therefore these quantities are independent of j. As seen in figures 2 and 3, both Gutzwiller and HFB provide essentially the same results. To understand the similarities between the HFB and the Gutzwiller ansatz we compute the *non-Gaussianity* for the

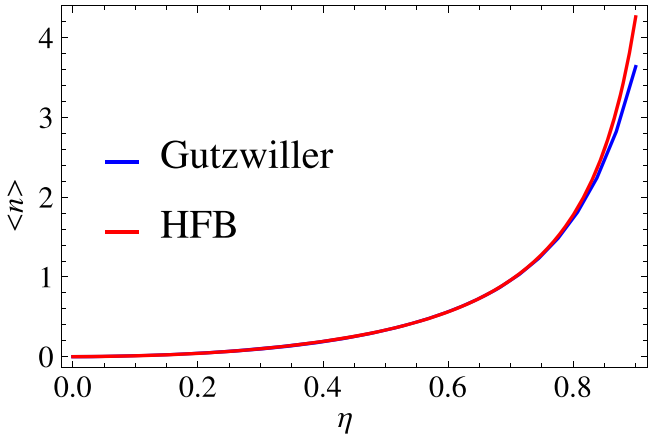

Figure 3. Steady state solution of $\langle n_j \rangle$ as a function of η for $U/J = 1.0$ for the HFB and the Gutzwiller ansatz. For both, HFB and Gutzwiller, we have chosen: $\omega = -2J$ and $q = 0$. The HFB result considers a linear array with 10 sites and periodic boundary conditions. For the Gutzwiller solution we have taken a photon cut-off $N_C = 60$.

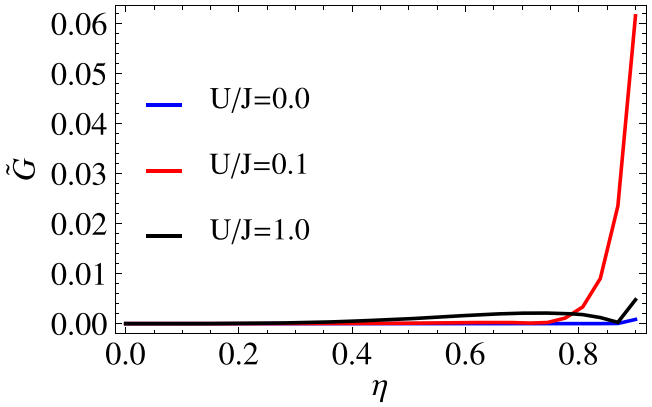

Figure 4. Non-Gaussianity $\tilde{G}$ for the Gutzwiller solution (equation (23)) as a function of η for different values of the ratio U/J. Plots are shown for: $U/J = 0$ (blue), $U/J = 0.1$ (red) and $U/J = 1.0$ (black). This solution corresponds to $\omega = -2J$, $q = 0$ and a photon cut-off $N_C = 60$.

Gutzwiller solution

$$\tilde{G} := \left| \left\langle a_j^\dagger a_j^\dagger a_j a_j \right\rangle - \left(2\left\langle a_j^\dagger a_j \right\rangle^2 + \left\langle \left(a_j^\dagger\right)^2 \right\rangle \left\langle a_j^2 \right\rangle - \left\langle a_j^\dagger \right\rangle^2 \left\langle a_j \right\rangle^2 \right) \right|, \tag{23}$$

where the last three terms come from computing the average $\langle a_j^\dagger a_j^\dagger a_j a_j \rangle$ with the Wick formula (4), i.e. assuming a Gaussian distribution. A value of $\tilde{G}$ greater than zero implies that the state is non-Gaussian. In figure 4 it is clearly appreciated that $\tilde{G}$ is always very small. Only in a small region for $\eta \cong 1$ and $U \cong 0.2$, $\tilde{G}$ differentiates from zero. Thus, both approximations are in excellent agreement for our model.

4.3.1. Transition to a thermal state. Once the approximations have been tested, let us now discuss the main physics occurring. First, we will consider the transition to a thermal state, pretty much like for the single site (cf section 4.2). In the limit of large U, we again rotate the state as in equation (15), having that $V a_j V^\dagger = \sum_n \mathrm{e}^{-\mathrm{i}2n_j Ut} |n_j\rangle\langle n_j| a_j$ (in the interaction picture with respect to the self-interaction term). The coupling $a_j^\dagger a_{j+1}$ + h.c. also averages to zero within the RWA argument. Therefore, in the large U limit the effective master equation is similar to (16) but summed over all the sites: $\partial_t \varrho = \frac{1}{2}\sum_l \left(2a_j \varrho a_j^\dagger - \{a_j^\dagger a_j, \varrho\} \right) + \frac{\eta^2}{2}\sum_j \left(2a_j^\dagger \varrho a_j - \{a_j a_j^\dagger, \varrho\} \right)$. The stationary state then reduces to a thermal state of uncoupled resonators with temperature given by (17).Further confirmation of the above picture within the HFB approximation comes from studying the X_{ij} terms in the thermodynamic limit ($N \to \infty$). Assuming translational invariance it is easy to see that we can obtain a closed set of equations for the diagonal terms of (6)

$$\mathrm{d}_t X_{ii} = -\left(1 - \eta^2\right) X_{ii} + \eta^2 \tag{24}$$

which generalizes (18) to the multi-site case. In a similar fashion, we obtain for the steady state solution

$$\langle a_i^\dagger a_i \rangle_{\varrho_{\mathrm{eq}}} = \frac{1}{\mathrm{e}^{\beta^* \omega} - 1}. \tag{25}$$

We stress that the latter is independent of U.

The appearance of this synthetic thermal state can be traced by computing the squeezing. For a thermal state this quadrature must equal 1/2 (coherent state). In figure 5 we can appreciate this transition. To understand it, we must recall the non-interacting case $U = 0$. There, the limit $\eta \to 1$ is a critical point where a couple of modes becomes a maximally entangled EPR state. In other words, the squeezing is infinite in this point. However, as soon as $U \neq 0$, ϱ_{eq} approaches a thermal state, with temperature given by (17), i.e., infinite as $\eta \to 1$. Therefore the squeezing becomes negligible as soon as $U \neq 0$ for such a big η. For smaller η the thermal state has a lower temperature and the squeezing survives for higher U.

4.3.2. No symmetry breaking. The non-dissipative BH model exhibits a $U(1)$ symmetry ($a_j \to a_j \mathrm{e}^{\mathrm{i}\phi}$). The latter is broken whenever the expectation value of a_j becomes different from zero (Mott insulator—superfluid transition [34]). In our case, equation (1) does not exhibit this symmetry, but it is symmetric under the parity transformation $a_j \to -a_j$. In the non-interacting case [15], the parity symmetry is never broken and $\langle a_j \rangle = 0$ always holds. For the single site (section 4.2) we already learnt that this was the case. We ask ourselves how this picture gets modified as soon as $U \neq 0$, and more sites enter the game.

In order to provide a strong argument, we are going to proceed again using the HFB approach and Gutzwiller ansatz. The set of parameters to investigate (ω, q, η, J, U) is huge. As we have already verified, the role of the on-site potential is to thermalize the state and therefore destroy the entanglement.

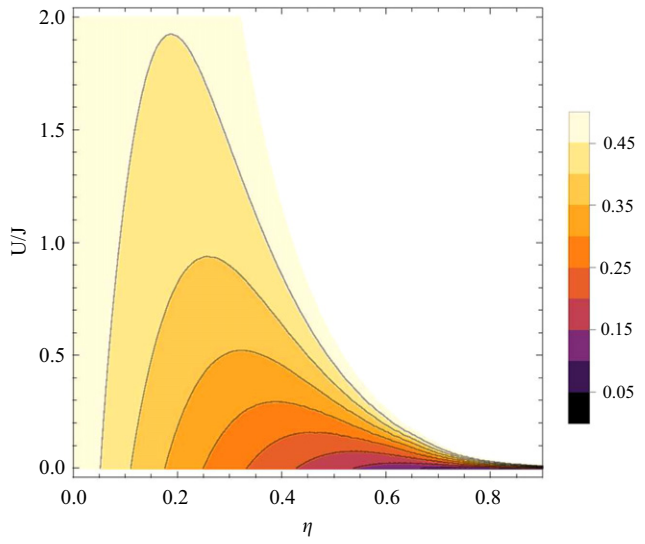

Figure 5. Squeezing (minimum eigenvalue of the covariance matrix) for a many-body array in the HFB approximation. The solution corresponds to a linear array with 10 sites and periodic boundary conditions. The parameters chosen were $\omega = -2J$ and $q = 0$. The white area in the plot corresponds to no squeezing—the eigenvalues of the covariance matrix are all greater or equal than 1/2 (according to the discussion in section 3.4).

Thus, a very favourable set of parameters is the one which maximizes the entanglement for $U/J = 0$. This is achieved by setting $\omega = -2J$ and $q = 0$ (that is, we impose that the zero momentum mode is maximally entangled (squeezed) in the absence of interaction). This seems reasonable due to the following argument. In the BH model without dissipation, the ground state in the regime $U/J \to \infty$ is a Mott insulator with a well defined number of excitations per site, thus, $\langle a_i \rangle = 0$. In the opposite limit $U/J \to 0$, the ground state is characterized by a product state with different particle number per site [35], therefore, $\langle a_i \rangle \neq 0$. The latter, the superfluid phase, corresponds to the presence of long-range correlations. Long-range ordering (divergent entanglement) in the present setup, is achieved for $U/J = 0$ and $\eta = 1$. Therefore, we could expect to find a broken symmetry around this configuration. However, we have always found that $\langle a_i \rangle = 0$ both in the HFB approximation and the Gutzwiller ansatz. Other parameter regimes were investigated but no symmetry breaking was found. Therefore, as we had anticipated, this model does not exhibit a phase transition.

5. Conclusions

We have studied the equilibrium statistics of a BH model with squeezed dissipation. To set it in a context, we mention that our model has no external driving competing with dissipation, as for example in [11–13]. The driving is, say, incoherent as introduced by the dissipators. In this sense, the physics discussed here is time-independent. It is the competition between the squeezing, generated via the dissipators, and the Hamiltonian which provides the equilibrium phases.

Our results can be summarized as follows. We have taken as a reference the limit of zero onsite repulsion ($U = 0$). This linear model was shown to be critical [7, 15]. In this work we have shown that as soon as $U \neq 0$ correlations shrink to zero. The stationary state approaches a trivial thermal state of uncoupled oscillators. The temperature of this synthetic state is proportional to the squeezing in the dissipators, given by equation (17). We emphasize that the dissipators (3) are not $U(1)$-symmetric, but they conserve the parity $a_j \to -a_j$. Furthermore, it has been argued that $\langle a_j \rangle = 0$ always. Thus, there is no condensation. Our findings were based on two approximations, the HFB and the Gutzwiller ansatz. The HFB is a Gaussian approximation (see section 3.1). The Gutzwiller assumes a factorized density matrix as explained in 3.2. These approximations can be understood as complementary: the HFB accounts for long distance correlators but it is approximate in the interacting part. On the other hand, the Gutzwiller can not catch long distance correlations but it is exact in the nonlinearities. The physics of the problem treated here provides an agreement between both approximations. The equilibrium state approaches the Gibbs state of uncoupled oscillators.

Acknowledgments

We acknowledge support from the Spanish DGICYT under Projects No. FIS2011-25167 and FIS2012-33022, by the Aragon (Grupo FENOL) and the EU Project PROMISCE. The authors would also like to acknowledge the Centro de Ciencias de Benasque Pedro Pascual for its hospitality.

Appendix A. Solutions for $\langle a \rangle$

We detail here our steps to demonstrate that $\langle a_i \rangle = 0$ for the single site case. The equations (within the HFB approximation) are:

$$\mathrm{d}_t \langle a \rangle = \left[-\mathrm{i}\omega - \frac{1}{2}\left(1 - \eta^2\right) + 2\mathrm{i}U \left|\langle a \rangle\right|^2 \right] \langle a \rangle - 2\mathrm{i}U \left(2\langle n \rangle \langle a \rangle + \langle a^2 \rangle \langle a \rangle^* \right) \tag{A.1}$$

and

$$\mathrm{d}_t \langle a^2 \rangle = \left[-\mathrm{i}(2\omega + 2U + 12U\langle n \rangle) - \left(1 - \eta^2\right) \right] \langle a^2 \rangle + 8\mathrm{i}U \left|\langle a \rangle\right|^2 \langle a \rangle^2 - \eta \mathrm{e}^{\mathrm{i}q} \tag{A.2}$$

with $\langle n \rangle = \eta^2/(1 - \eta^2)$ as given by equation (18). This is a nonlinear set of equations, we do not known how to solve the general case analytically. We are interested in the equilibrium solution. Therefore we are searching for solutions $\partial_t \langle a \rangle_{\varrho_{\mathrm{eq}}} = 0$ and $\partial_t \langle a^2 \rangle_{\varrho_{\mathrm{eq}}} = 0$.

We realize that $\langle a \rangle_{\varrho_{\mathrm{eq}}} = 0$ is always a solution of the system, indeed for $U = 0$ it is the only solution. We want to check if $\langle a \rangle_{\varrho_{\mathrm{eq}}} \neq 0$ is also solution. Assuming continuity, we

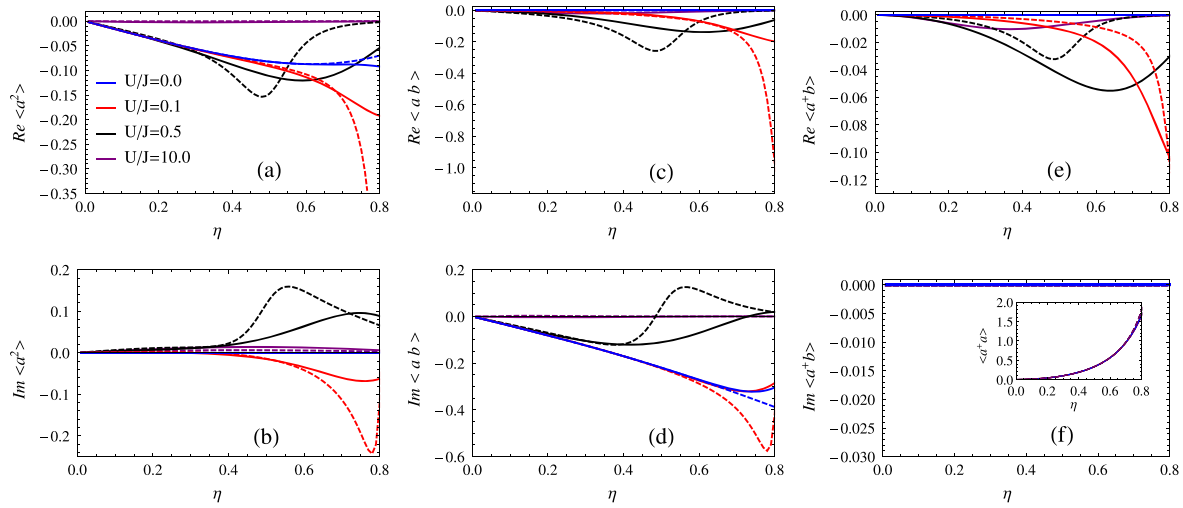

Figure A1. Two site ($N = 2$) case (a) real and (b) imaginary part of $\langle a^2\rangle$, (c) real and (d) imaginary part of $\langle ab\rangle$, (e) real and (f) imaginary part of $\langle a^\dagger b\rangle$ (inset: number of photons in one of the cavities) all of them as a function of η for different values of the ratio U/J. We compare the full numerical solution (solid line) and the HFB approximation (dashed line). For both, numerical and approximate solutions, we have considered the following parameters: $\omega = 0$ and $q = \pi$ (this choice maximizes the entanglement at $U = 0$ in the case of having only two sites). The numerical solution have been performed with a photon cut-off of $N_C = 20$.

suppose that for $U \neq 0$ exists $\langle a\rangle_{\varrho_{\rm eq}} = \epsilon$ with $|\epsilon| << 1$. Then, we linearize (A.1) and (A.2) discarding the terms with $|\langle a\rangle|^2$. Proceeding in this way, (A.2) becomes a closed equation for $\langle a^2\rangle_{\varrho_{\rm eq}}$ with solution given by (22). Formula (22) is introduced in (A.1) obtaining a linear set for both the real (R) and imaginary (I) parts of $\langle a\rangle_{\varrho_{\rm eq}}$:

$$\begin{pmatrix} 2U\langle a^2\rangle^{\rm I}_{\varrho_{\rm eq}} - \dfrac{1-\eta^2}{2} & -4U\langle n\rangle_{\varrho_{\rm eq}} - 2U\langle a^2\rangle^{\rm R}_{\varrho_{\rm eq}} \\ 4U\langle n\rangle_{\varrho_{\rm eq}} - 2U\langle a^2\rangle^{\rm R}_{\varrho_{\rm eq}} & -2U\langle a^2\rangle^{\rm I}_{\varrho_{\rm eq}} - \dfrac{1-\eta^2}{2} \end{pmatrix} \times \begin{pmatrix} {\rm Re}\left[\langle a\rangle_{\varrho_{\rm eq}}\right] \\ {\rm Im}\left[\langle a\rangle_{\varrho_{\rm eq}}\right] \end{pmatrix} = 0. \tag{A.3}$$

In our search for a non-trivial solution, we force the determinant of the above matrix to be zero obtaining the condition:

$$\left|\left\langle a^2\right\rangle_{\varrho_{\rm eq}}\right|^2 = 4\langle n\rangle^2_{\varrho_{\rm eq}} + \frac{\eta^4}{16U^2\langle n\rangle^2_{\varrho_{\rm eq}}}. \tag{A.4}$$

A graphical solution of the above shows that this condition never holds. Indeed we can see that $4\langle n\rangle^2_{\varrho_{\rm eq}} + \frac{\eta^4}{16U^2\langle n\rangle^2_{\varrho_{\rm eq}}} > |\langle a^2\rangle_{\varrho_{\rm eq}}|^2$ always.

This argument was also tested numerically, searching for any solution of the full nonlinear set of equations (A.1) and (A.2), not only non-vanishing continuations of $\langle a\rangle_{\varrho_{\rm eq}} = 0$. In the explored range $0 < U < 10$ and $0 < \eta < 0.99$ the only solution we found was the trivial $\langle a\rangle_{\varrho_{\rm eq}} = 0$. If we perform a mean field approximation to the many-body equations, i.e. replacing the hopping term by $J(\langle a_j^\dagger\rangle a_j + \text{h.c.})$, the problem is reduced to the single site case already discussed. The only difference is that the onsite frequencies get shifted by $\omega \to \omega + J$. Then, in mean field approximation and within the HFB approximation no broken symmetry is expected.

Appendix B. Two site case: a critical analysis of the HFB approximation

In this appendix we test the HFB for the dimer ($N = 2$). We compute the second moments both numerically and within the HFB. We plot the comparison in figure (A1). Some comments are relevant. Appealing to our experience with the single site, the population in each site diverges as $\eta \to 1$ in equation (18) (see also figure A1 (f)). Therefore, our numerics fail in this limit. Our accuracy tests do not permit to show results for $\eta > 0.8$. In this case we observe that for high nonlinearities ($U \cong 0.5$) the HFB is not accurate at intermediate values of η ($0.4 < \eta < 0.8$). For higher values of η we expect things to get better (in fact, the HFB results clearly show this behavior). A similar behavior was found for the single site case. This can be understood on the grounds of the synthetic thermal state approach developed for it. For low values of the nonlinearity and high values of η, the steady state exhibited the behavior of a thermal state with large temperature $\beta^* \sim -\ln\eta$. Increasing the value of U means that $\varrho_{\rm eq}$ approaches a thermal state $\sim e^{\beta\omega\sum a_j^\dagger a_j}$ which is gaussian (cf section 4.2).

References

[1] Bloch I, Dalibard J and Zwerger W 2008 *Rev. Mod. Phys.* **80** 885–964
[2] Houck A A, Türeci H E and Koch J 2012 *Nat. Phys.* **8** 292–9
[3] Tomadin A, Diehl S and Zoller P 2011 *Phys. Rev.* A **83** 013611

[4] Tomadin A, Diehl S, Lukin M D, Rabl P and Zoller P 2012 *Phys. Rev.* A **86** 033821
[5] Horstmann B, Cirac J I and Giedke G 2013 *Phys. Rev.* A **87** 012108
[6] Diehl S, Tomadin A, Micheli A, Fazio R and Zoller P 2010 *Phys. Rev. Lett.* **105** 015702
[7] Eisert J and Prosen T 2010 arXiv:1012.5013
[8] Jin J, Rossini D, Fazio R, Leib M and Hartmann M J 2013 *Phys. Rev. Lett.* **110** 163605
[9] Ruiz-Rivas J, del Valle E, Gies C, Gartner P and Hartmann M J 2014 arXiv:1401.5776
[10] Jin J, Rossini D, Leib M, Hartmann M J and Fazio R 2014 *Phys. Rev.* A **90** 023827
[11] le Boité A, Orso G and Ciuti C 2013 *Phys. Rev. Lett.* **110** 233601
[12] Grujic T, Clark S R, Jaksch D and Angelakis D G 2013 *Phys. Rev.* A **87** 053846
[13] Boité A L, Orso G and Ciuti C 2014 arXiv:1408.1330
[14] Dalla Torre E G, Otterbach J, Demler E, Vuletic V and Lukin M D 2013 *Phys. Rev. Lett.* **110** 120402
[15] Quijandría F, Porras D, García-Ripoll J J and Zueco D 2013 *Phys. Rev. Lett.* **111** 073602
[16] Jaksch D, Bruder C, Cirac J I, Gardiner C W and Zoller P 1998 *Phys. Rev. Lett.* **81** 3108–11
[17] Lewenstein M, Sanpera A and Ahufinger V 2012 *Ultracold Atoms in Optical Lattices: Simulating Quantum Many-Body Systems* (Oxford: Oxford University Press)
[18] Cazalilla M, Citro R, Giamarchi T, Orignac E and Rigol M 2011 *Rev. Mod. Phys.* **83** 1405–66
[19] Leib M and Hartmann M J 2010 *New J. Phys.* **12** 093031
[20] Rivas Á and Huelga S 2011 *Open Quantum Systems: An Introduction (Springer Briefs in Physics)* (Berlin: Springer)
[21] Breuer H P and Petruccione F 2002 *The Theory of Open Quantum Systems* (Oxford: Oxford University Press)
[22] Pachon L A, Triana J F, Zueco D and Brumer P 2014 arXiv:1401.1418
[23] Kepesidis K V and Hartmann M J 2012 *Phys. Rev.* A **85** 063620
[24] Pudlik T, Hennig H, Witthaut D and Campbell D K 2013 *Phys. Rev.* A **88** 063606
[25] Köhler T and Burnett K 2002 *Phys. Rev.* A **65** 033601
[26] Rey A M, Hu B L, Calzetta E, Roura A and Clark C W 2004 *Phys. Rev.* A **69** 033610
[27] Holland M, Park J and Walser R 2001 *Phys. Rev. Lett.* **86** 1915–8
[28] Proukakis N P, Burnett K and Stoof H T C 1998 *Phys. Rev.* A **57** 1230–47
[29] Griffin A 1996 *Phys. Rev.* B **53** 9341–7
[30] Takayoshi S, Sato M and Furukawa S 2010 *Phys. Rev.* A **81** 053606
[31] Kevrekidis P 2009 *The Discrete Nonlinear Schrödinger Equation* (Berlin: Springer)
[32] Tan S 2002 *A Quantum Optics Toolbox for Matlab 5*
[33] Simon R, Mukunda N and Dutta B 1994 *Phys. Rev.* A **49** 1567–83
[34] Sachdev S 2011 *Quantum Phase Transitions* 2nd edn (Cambridge: Cambridge University Press)
[35] Rokhsar D S and Kotliar B G 1991 *Phys. Rev.* B **44** 10328–32